Why Are Collision Induced Rotational Distributions Unresponsive to Kinematic Differences?

Suzanne Clare, Alison J. Marks,† and Anthony J. McCaffery*

School of Chemistry, Physics and Environmental Sciences, University of Sussex, Brighton BN19QJ, U.K.

Received: December 13, 1999; In Final Form: April 13, 2000

An unanswered question in collision-induced rotational transfer (RT) centers on the *similarities* that characterize the distributions of Δj states despite very large differences in mass and chemical composition of collision partners (Clegg, S. M.; Burrill, A. B.; Parmenter, C. S. *J. Phys. Chem. A* **1998**, *102*, 8447). We show these observations to be consistent with a kinematic model whose *mechanism* is the conversion of linear momentum of relative motion into rotational angular momentum (AM) via a torque arm (b_n) of molecular dimension. The mechanism operates strictly within boundary conditions set by energy conservation and, in certain kinematic circumstances, the range of b_n values that may be accessed is constrained. These constraints are particularly marked when initial rotor state, $j_i \gg 0$ and when reduced mass (μ) is large. The occurrence of constraints is clearly seen in velocity−AM plots and the reduction of b_n that results is readily quantified. Insights obtained from velocity−AM plots for $j_i > 0$ and large μ are confirmed through multi hard ellipsoid Monte Carlo calculations. The analysis presented here indicates that the energy corrected form of the IOS scaling relation does not adequately represent the RT mechanism for $j_i \neq 0$ and introduces poorly defined parameters that appear unnecessary for a full description.

Introduction

Collisions are at the very heart of chemistry and an understanding of the mechanism controlling the outcomes of inelastic and reactive collisions is central to this subject. Research into collision-induced processes is not as intensive as was the case a few years ago but this should not be taken to imply that the subject is well understood even for the simplest of inelastic events, rotational transfer (RT), as the review of Schiffman and Chandler[1] makes abundantly clear. Although quantum scattering theory and its variants yields results which often agree well with experiment, little physical insight is obtained in these computer-intensive methods. Furthermore, unexplained collisional transfer phenomena in atom−molecule and molecule−molecule collisions are sufficiently numerous[1] to suggest that the underlying physics is yet to be fully revealed.

In a series of recent publications, we have introduced a simple and physically transparent model of RT[2,3] and have applied this successfully to a range of collision-induced processes including vibration−rotation transfer (VRT)[4,5] and quasiresonant vibration−rotation transfer (QRT).[6,7] The *mechanism* consists of momentum transfer within constraints or *boundary conditions* set by energy conservation. In this kinematic model, momentum of relative motion is converted into rotational angular momentum via an effective impact parameter (b_n) at the hard wall of the intermolecular potential and/or into linear momentum of vibration. A hard ellipse representation of the parameters of linear-to-angular momentum interconversion is shown in Figure 1. The model adopted is sufficiently simple that unresolved issues in collisional RT and VRT may be investigated without the introduction of additional assumptions.

The "natural" or commonly observed distribution of rotational states in pure RT in a diatomic molecule is "exponential-like"

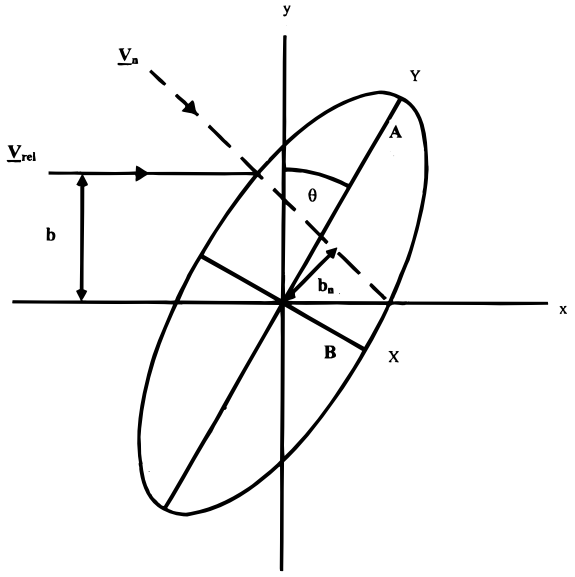

Figure 1. Parameters of the hard ellipse model that forms the basis of the multi hard ellipsoid Monte Carlo calculations reported here and defines the effective impact parameter b_n (or torque arm) about which linear momentum is converted to angular momentum. v_n is the surface normal velocity component, *A* and *B* are semimajor and semiminor ellipse axes respectively, *b* is the impact parameter, and v_r is the initial relative velocity.

as first noted by Polanyi and Woodall.[8] Extensive empirical studies[9] showed this distribution is more accurately described as an inverse power dependence on Δj, the transferred angular momentum (AM). In the angular momentum theory of RT[2,3] this dependence originates in the probability density of reduced impact parameter $P(b_n)$ which in the model represents an average of radial and angular (repulsive) anisotropies and is shown to have the functional form $b_n^{-\gamma}$.[3] A transfer function derived from

* Author for correspondence.
† School of Pharmacy, University of Bradford, Bradford.

10.1021/jp994392b CCC: $19.00
Published on Web 07/13/2000

the AM theory[3] has this representation of $P(b_n)$ as its core and is an excellent predictor of RT rate constants for a wide range of collision systems. Thus, the linear-to-angular momentum (LM → AM) mechanism contains at least a substantial fraction of the physics needed to describe fully the RT process.

In this model, energy conservation sets boundary conditions within which the LM → AM mechanism must operate. Much RT takes place with little in the way of such constraints and the process is characterized by what generally are the largest of overall cross sections observed in inelastic transfer. In some instances, however, energy constraints have a profound influence on RT distributions and this is most dramatically displayed when vibration and rotation transfer take place simultaneously. We have shown that in these cases, the mechanism remains unaltered and the rich variety of behavior found in VRT and QRT originate in changes in the energy conservation boundary conditions.[4−7] We note at this point that the mechanism is also constrained by the need to yield *quantized* molecular eigenstates and with this as a further condition, accurately predicts the outcome of the most sophisticated of molecular dynamics experiments, namely velocity- and state-resolved angular distributions.[10]

In VRT[4,5] and, more spectacularly, QRT[6,7] the collision-induced rotational state distributions are very different from the exponential-like form that characterizes unconstrained RT. Despite this, we have presented arguments to show that each is in fact no more than a modified form of the natural exponential-like decay in Δj, the modifications originating in constraint induced restrictions on the maximum permissible value of b_n. Kinematic conditions also exist under which constraints reduce the efficiency of RT *without changing the exponential-like appearance of the collisional distribution*. We address this particular circumstance here, and in so doing, illustrate the ways in which energy conservation boundary conditions may introduce constraints on the *range* of the effective impact parameter. We confirm this view of the influence of kinematic factors on RT rate constants using multiellipsoid Monte Carlo calculations.

Kinematic models are advantageous in that calculations of at least rule-of-thumb accuracy may be performed using readily available quantities such as atomic and molecular masses, atomic radii and, crucially for the AM model, the diatomic bond length. This latter quantity (or half this latter quantity to be more precise) is found frequently, from experiment, to be the maximum value of b_n, the effective impact parameter or torque arm for conversion of linear to angular momentum. A growing weight of experimental evidence indicates that kinematic factors determine the outcome of nonreactive collisions. Parmenter and co-workers[11,12] report that inelastic transfer in the glyoxal molecule bears little relation to the intermolecular potential for a wide range of collision partners. Particularly convincing is their data obtained using partners of identical mass but of very different chemical constitution.

A number of important questions still remain in the field of RT and of vibrotational transfer (VRT), one of which was posed recently by Clegg et al.[12] These authors surveyed RT data for the diatomics I_2, Na_2, Li_2, NO, HF and CN obtained using a range of rare gas atoms as collision partners and concluded,[12] "...common cross-section distributions among the rare gas partners appear to be the rule rather than the exception". On the surface, this finding seems at odds with a mechanism based on LM → AM interconversion in which collision generated AM is linearly dependent on reduced mass. In this publication, we seek to answer the question implicit in the work of Clegg et al.[12] namely, *why, in a process dominated by kinematics is there so little change when for example the mass of the collider species changes by more than an order of magnitude?*. In this work, we show that this observation is an important clue to the key role played by the energy conservation boundary condition, the mechanism of LM → AM remaining unchanged throughout.

In a series of recent publications,[4−7] we have demonstrated that plots of relative velocity (v_r) versus change in rotational AM (Δj) provide a very powerful means of analyzing the kinematics of RT and VRT. These $v_r-\Delta j$ plots give a very useful rule-of-thumb guide to the location of RT peaks and distributions Simple Monte Carlo computational routines based on the physical principles outlined above give the full distribution. Velocity−AM plots were first introduced by Besley et al.[13] and their value lies in their ability to display the LM → AM mechanism in the same coordinates as the energy conservation boundaries. Furthermore, velocity distributions may also be shown on this same diagram and thus all elements of the kinematics of collision are represented.

In the next section we describe the basis of the velocity−AM plots in more detail and show that in certain kinematic circumstances, the LM → AM mechanism must be modified in order to meet restrictions imposed by energy conservation. These modifications may be made quantitatively in straightforward fashion but in effect they represent restrictions upon the trajectories which may contribute to collision induced state change, a process we have termed *stereokinematics*.[4] In the cases we describe here of pure RT over a range of kinematic conditions these restrictions cause the RT rate constants to appear very similar in form to one another as e.g. collision partner mass increases. This phenomenon becomes greatly magnified as initial rotor state increases and the reasons for this are clearly revealed in velocity−AM plots. Predictions based on the $v_r-\Delta j$ diagrams are confirmed using multi hard ellipsoid (MHE) Monte Carlo trajectory calculations of RT probabilities for $(A)^1\Sigma_u^+$ Na_2, a system for which much experimental data exists.[14]

Velocity−Angular Momentum Plots

We have stressed[4−7,13] the importance of the *threshold* or channel opening velocities which are readily displayed through $v_r-\Delta j$ plots. These illustrate the kinematics of the molecule−collider interaction in a way that reveals the underlying physics of the collision-induced quantum state change and represent a very useful first step in the analysis of the system under study. The diagrams are a graphical representation of the threshold conditions for conversion of relative velocity of collision into *change of* angular momentum (Δj) for the following processes:

(i) conversion of kinetic energy of relative motion to change of rotational energy via the relation

$$\Delta j = -j_i + \frac{\sqrt{(2Bj_i)^2 + 2B\mu(v_r^{th})^2}}{2B} \qquad \text{(E equation)} \quad (1)$$

Here B is the rotational constant for the diatomic species, μ the reduced mass of the collision pair and v_r^{th} the channel opening relative velocity. This equation, given here for the case $j_i \neq 0$, is referred to in what follows as the E equation since it represents the onset of conditions that meet energy conservation.

(ii) conversion of relative velocity into change of rotational AM via an effective impact parameter or torque arm (b_n)

$$\Delta j = \mu v_r^{th} b_n^{max} \qquad \text{(A equation)} \quad (2)$$

In this expression, b_n^{max} is the *maximum* value of torque arm

about which LM → AM is effected. Besley et al.[13] have demonstrated that this represents the onset of Δj channel opening through *forward* scattering via the LM → AM mechanism and is referred to in the following as the A equation.

(iii) The expression for simultaneous energy and AM conservation for the case $j_i > 0$ is considerably more complex than that for $j_i = 0$ and is given below. It is used in the MHE Monte Carlo calculations reported below and we refer to it as the (E + A) equation.

$$j_f = \frac{1}{(I + \mu(b_n^{\max})^2)} \times [(l_i + j_i)I \pm \sqrt{(l_i^2 I^2 + \mu(b_n^{\max})^2 j_i(j_i\mu(b_n^{\max})^2 - 2Il_i)}] \quad \text{(E + A) equation} \quad (3)$$

Here I is the moment of inertia of the diatomic molecule, j_i, j_f are initial and final rotor states, respectively. l_i is the orbital AM available for transfer into molecular rotation at the point of impact and is defined as $l_i = \mu v_r^{\text{th}} b_n^{\max}$.

In many circumstances $b_n^{\max}$ is found to be close to half the bond length (HBL) (for homonuclear diatomic molecules) and thus the model emphasizes the significance of the physical shape of the molecule. The value of b_n will in general be related to the repulsive anisotropy of the intermolecular potential and HBL is a reasonably accurate approximation to this for the zero potential energy contour. In this work we shall find that energetic constraints frequently restrict the maximum value of b_n to be less than HBL. Note that a simpler version of the (E + A) equation (that for $j_i = 0$) is given in earlier papers in this series.

The probability density for the conversion of linear momentum of relative motion into rotational AM is the transfer function for RT given by Osborne and McCaffery,[3]

$$P(j_f|j_i)dj_f = C\int_0^{b_n^{\max}} P(l|b_n)\,\delta(|E_{\text{tot}} - E'_{\text{tot}}|) \times \delta(|J_i - J_f|)b_n\,\mathrm{d}b_n\,\mathrm{d}j_f \quad (4)$$

Note here the key role played by $b_n^{\max}$ in the integral of eq 4. Restrictions on the maximum value of b_n will have an impact on the probability (i.e., rate constant or cross section) for the process $j_i \rightarrow j_f$. Also of note in eq 4 is the general expression of energy conservation which is given explicitly in eq 1. Equation 4 predicts an inverse power dependence of RT probabilities in Δj, a consequence of functional form of the probability density of b_n.[3] This in turn is related to the repulsive anisotropy averaged over both radial and angular coordinates.

Besley et al.[13] discuss the relevance of eqs 1−3 and the value of $v_r^{\text{th}}-\Delta j$ plots in the analysis of final state and angular distributions in rotationally inelastic scattering. Equation 2 is particularly significant in this context since it represents the velocity at which each Δj channel is opened for forward scattering. Equation 3 on the other hand permits forward and backward scattering (and from which channel opening velocity for the latter may be calculated). RT predominantly occurs under circumstances in which collision-induced transfer is a small fraction of the initial relative linear momentum and thus forward scattering characterizes much of this inelastic process.

As mentioned above eqs 1−3 are referred to as the E equation (eq 1), the A equation (eq 2) and the (E + A) equation (eq 3). It will be seen below that significant changes take place in the relative positions of the E and the A relationships in $v_r-\Delta j$ space as kinematic conditions change. Again we emphasize that in this model the E equation acts only to delineate the region within which energy conservation applies and is that in which the LM → AM mechanism must operate. The result of this may, in certain circumstances, set constraints upon the operation of the mechanism and thus require modification of the A equation. These changes are readily calculated so that the mechanism operates entirely within the boundaries of energy conservation. We show below that this effect is particularly associated with the situation in which $j_i > 0$ and is exacerbated by the presence of a heavy collision partner.

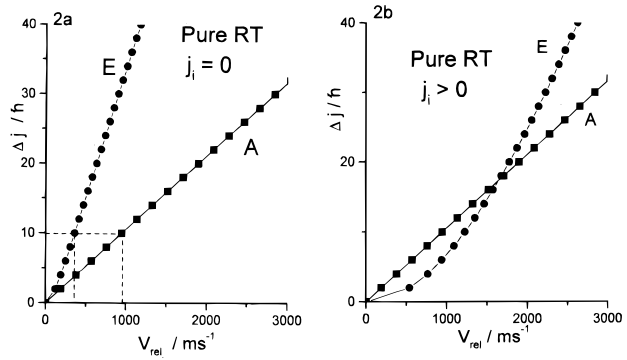

Figure 2. Two generic forms of velocity−AM diagrams in which eqs 1 and 2 are plotted on common axes. The first of these (Figure 2a) is found, e.g., in heavy diatomic-light atom collisions when $j_i \simeq 0$. In this case, for all Δj, the channel opening velocity for the LM → AM mechanism (represented by the A plot where $b_n^{\max}$ = HBL) exceeds that of the energy conservation boundary condition (E plot). In such circumstances full $b_n^{\max}$ is available for all channels and RT has optimum efficiency. Figure 2b. is associated with light diatomic-heavy atom kinematics and/or $j_i \gg 0$. Here the mechanism is *constrained* by the energy conservation relation and must be modified with (channel-dependent) restrictions on the maximum value of b_n. This results in marked loss of efficiency in the RT process, particularly for low Δj.

The use of velocity−AM plots in analysis of collision induced processes is relatively new and in order to illustrate their power in identifying the underlying physical process, we describe two generic forms (of the four thus far identified)[5,7] of these plots which are of particular relevance to pure RT. Figure 2 shows $v_r-\Delta j$ plots for two kinematic circumstances commonly found in RT. Figure 2a characterizes RT for the heavy diatomic, light collision partner combination when initial rotor state $j_i \simeq 0$. Figure 2b is more commonly found when the collision reduced mass is large and when $j_i \gg 0$.

In the kinematic circumstances depicted in Figure 2a, the channel opening relative velocity calculated from the E equation (eq 1) is lower than that predicted through the A equation (eq 2) for all values of Δj. The A plot shown assumes $b_n^{\max}$ = HBL. The mechanism (represented by the A plot) is unconstrained by energy conservation conditions for all Δj with all values of b_n available up to its maximum permissible from the repulsive anisotropy of the intermolecular potential. Thus, for $\Delta j = 10$, e.g., the mechanism of LM → AM operates from 950 ms^{-1} upward (despite this channel having opened on energy grounds at 375 ms^{-1}. As discussed briefly above, and in more detail by Besley et al.,[13] the mechanism referred to and quantified in the A relation is the threshold condition for channel opening by *forward* scattering.

Figure 2b displays a situation where, for some Δj channels, the channel opening velocity required by the E equation is now higher than that required by the (unmodified) A equation. The LM → AM mechanism is now *constrained* by the energy conservation condition. However, we note that eq 2 expresses AM change as occurring via a torque arm of length $b_n^{\max}$ set initially at HBL for the molecule under consideration. The plot of Figure 2b indicates that the LM → AM, mechanism is now

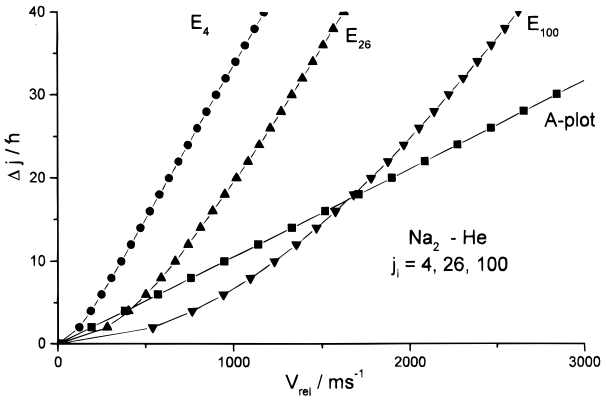

Figure 3. Velocity−AM plots for Na_2*−He collisions. *Note that the plots represent threshold or channel opening conditions*. The graph shows the E equation (eq 1) for $j_i = 4$, 26, 100$\hbar$. The A equation is plotted with b_n^{max} = HBL and is the same for all j_i. At low Δj (for j_i = 26, 100) the A equation, as plotted here, falls partially in a v_r−AM region that does not meet the requirements of energy conservation and must be modified in the manner described in the text.

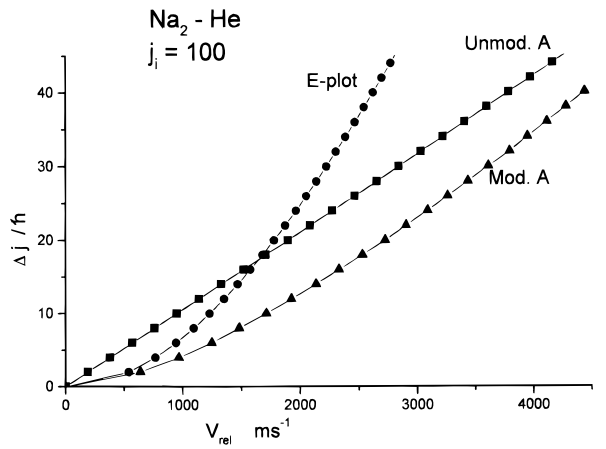

Figure 4. Velocity−AM plot for Na_2* ($j_i = 100$)−He collisions. The E and unmodified A plots are as shown in Figure 3. The modified A plot represents channel-opening velocities for the operation of the LM → AM mechanism adapted to meet the requirements of energy conservation in the manner described in the text.

restricted in range that b_n may take and is limited to some maximum value, one obtained by simultaneously solving the A and E expressions. The figure also makes clear that the maximum values of b_n will differ for each Δj channel. This new maximum value will be smallest for low values of Δj and in eq 4 there will be severe constraints at low Δj on the range of b_n that may be sampled. This, in effect, becomes a restriction on the permitted trajectories for populating an individual channel. Thus, the *outcome* or final Δj state sets the conditions on acceptable collision trajectories that will lead to the opening of that channel.

With this brief introduction to the use of velocity−AM diagrams, we next consider the effect of changing kinematic conditions on RT probabilities.

Effect of Initial Rotor State

Figures 3−5 show plots of the E and the A equations for j_i = 4, 26, and 100$\hbar$ for collisions of Na_2* with He (Figure 3 and 4) and Xe (Figure 5). We begin by discussing the curves for Na_2*−He and in Figure 3, the E equation is plotted for collision-induced Δj transitions occurring from three initial j states. Also shown is the A equation with b_n^{max} = HBL. The E plots

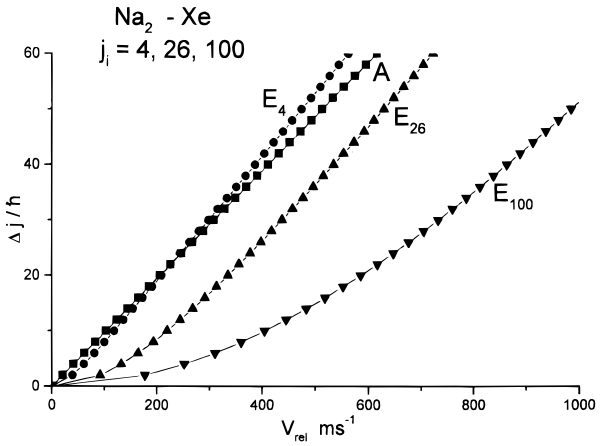

Figure 5. As for Figure 3 but now the data plotted are for Na_2* collisions with Xe. Note that for Xe as collision partner, *all* j_i shown here are affected by the requirements of energy conservation and the LM → AM mechanism must be modified to take account of this.

become curved at low Δj when $j_i \neq 0$ an effect which is more pronounced as j_i increases. The A plot is the same for all j_i *if we assume* b_n^{max} *to be HBL for each case*. As discussed above, this assumption requires modification when $j_i \gg 0$.

Consider first the E plot for $j_i = 4\hbar$ and its relationship to the A plot. This is very similar the case shown in Figure 2a and we expect the LM → AM mechanism (b_n^{max} = HBL) to be unconstrained for all v_r. This represents a kinematic situation of maximum efficiency for the RT process since the integral of eq 4 may range up to the full b_n^{max} available.

The plot for $j_i = 26\hbar$ has some curvature at low Δj and the relative positions of A and E plots in v_r−Δj space now begin to resemble Figure 2b. In this case the assumption of HBL for the maximum value of b_n is untenable on grounds of energy conservation. The LM → AM mechanism is readily made to conserve energy and the manner in which this might be accomplished is evident in the figure. Reduction of the maximum value of b_n (and hence the slope of the line) can bring the A plot into a region of v_r−Δj space such that it now resembles Figure 2a. The new (reduced) maximum b_n is readily calculated from eqs 1−3. In addition, the extent of this reduction will vary depending on the Δj channel (because of the curvature in the E plot), and will have most impact on low Δj. Reductions in RT efficiency will result from these restrictions on b_n since, as described above, eq 4 becomes limited in range of integration over b_n and this restricts trajectories that may contribute to RT into particular channels.

For $j_i = 100\hbar$, E and A relationships now closely resemble the pattern displayed in Figure 2b and major reductions in RT efficiency may be anticipated in this case. Reductions in the maximum torque arm length are again required to maintain the AM mechanism within the bounds of energy conservation. Furthermore, because the energetically allowed channel opening velocities are much higher than those predicted by the A equation, the maximum value of b_n must be reduced very markedly particularly for low values of Δj. These new b_n values are straightforwardly calculated and are presented for each channel in Table 1. From these, revised A equation channel opening v_r values may be calculated and are shown as the *modified* A relation, along with the E plot and the unmodified A plot in Figure 4. Following the arguments presented above, constraints on the maximum b_n will have a major impact on RT efficiency since the number of successful trajectories is much

TABLE 1: Upper Limits to b_n^{max} for Specified Δj Channels for Pure RT in (A)Na_2*($j_i = 100$)−He Collisions

$\Delta j/\hbar$	b_n^{max}/Å	$\Delta j/\hbar$	b_n^{max}/Å
2	0.53	22	1.28
4	0.70	24	1.31
6	0.81	26	1.35
8	0.91	28	1.38
10	0.99	30	1.40
12	1.06	32	1.43
14	1.11	34	1.46
16	1.16	36	1.48
18	1.20	38	1.50
20	1.24	40	1.52

reduced, although the final distribution is expected to be exponential-like in nature.

Effect of Reduced Mass

Velocity−Δj plots ($j_i = 4$, 26, 100$\hbar$) for Na_2*−Xe collisions (Figure 5) illustrate the impact of increased collision partner mass on the kinematic relationships. The E relation now appears to determine channel opening velocities to at least some degree for each of these j_i and the A relation must be modified in order that it may operate entirely within a framework of energy conservation. The influence of increasing j_i is greatly amplified when Xe is the partner. For $j_i = 100\hbar$, large reductions to the range of b_n are required to maintain the AM mechanism within the bounds of energy conservation. The modified A relation in this case (not shown in the figure) has pronounced curvature at low Δj and lies to the high v_r side of the E relation for all Δj. As discussed above, these restrictions in available b_n values in collision will cause a very marked reduction in RT cross sections from $j_i = 100$.

The modified maximum values of b_n may be used in calculations of RT probabilities using the probability density expression of eq 4, or as shown here and in ref 4, through hard ellipsoid Monte Carlo simulation calculations of RT (or VRT) probabilities. The physical origin of the reduced mass effect in increasing the dominance of the E constraint can be seen from the plots in Figures 3 and 5. As reduced mass increases, each channel opening velocity shifts to lower values linearly with mass in the case of the A equation but as $\sqrt{\mu}$ for the E expression with the consequences described in the foregoing paragraphs.

Multiellipsoid Monte Carlo Calculations

In this section we use more quantitative methods to demonstrate the effect of changing kinematic factors on state-to-state RT cross sections. The physically transparent hard ellipse (HE) model displayed in Figure 1 and first formulated by Bosonac[15] is the basis of the approach in which LM → AM is calculated explicitly. The method was developed further by Kreutz and Flynn[16] using a Monte Carlo simulation of collision trajectories together with a three-dimensional ellipsoid representing the repulsive wall of the intermolecular potential. This model was modified further by Marks[17] who introduced a multi hard ellipsoidal (MHE) representation to simulate the "soft" repulsive wall of the intermolecular potential. Marks showed that the exponential-like fall of pure RT cross sections in $X^1\Sigma_g^+$ Na_2−He could be reproduced quantitatively by using at least four ellipsoids constructed from the published potential.[18] Marks further noted[17] that a single ellipsoid failed to reproduce the exponential-like fall of RT cross sections found experimentally and theoretically[18]

Note that in this work we make no attempt at quantitative reproduction of RT cross sections for any of the systems under consideration. Our objective is to assess the changes in RT behavior that are brought about as j_i and μ are varied and thus a representation of a model potential is perfectly satisfactory for this purpose. Korsch and Ernesti note that "...amazingly simple models allow very precise description of experimental RT results" and comment that the critical factor in the potential is the repulsive anisotropy.[19]

The basis for our model potential is that reported by Schinke et al.[18] for $X^1\Sigma_g^+$ Na_2−He. These authors have published an analytical form of the potential function and this was scaled so as to give zero contour for the (A) state that matches the b_n^{max} value extracted from the fit to (A) state RT data.[3] This is very close to HBL for the excited Na_2 molecule. The anisotropy of (A)Na_2* is particularly large, which of course is the origin of the extensive RT in this species. We emphasize that this model potential is not intended as an accurate representation of any of the collision pairs discussed here. Indeed, scaling of both 0° and 90° contours of the $X^1\Sigma_g^+$ Na_2−He potential might be seen as unphysical since on excitation to the (A) state, it is the bond length that extends. Nevertheless, calculations based on the $X^1\Sigma_g^+$ Na_2−He potential as a series of ellipsoids is known to reproduce the RT cross sections *quantitatively* for this system and a representation of the excited state scaled-up to give the correct b_n^{max} will certainly reproduce the principal features of the (A) state RT behavior.

In a previous section we utilized velocity−AM plots to illustrate the physical processes at work when kinematic factors are changed. The principal effect is that the range of accessible b_n values is reduced and modified maximum values of b_n are readily calculated for incorporation into the transfer function of eq 4. However, in the Monte Carlo method, eq 3 (or its variant for $j_i = 0$) is used throughout so that energy conservation is automatically imposed while calculating LM → AM for each trajectory. In this method therefore, trajectory restrictions consequent on the b_n reduction are automatically introduced provided that the representation of the potential is sufficient for the purpose of the calculation. This latter point is relevant here. In a study of VRT in CO_2 we found that a single ellipsoid was able to reproduce experimental results only when the b_n reductions were incorporated.[4]

In (X)Na_2−He, Marks[17] found that a single ellipsoid cannot adequately reproduce the low Δj region of the RT distribution. Korsch and Schinke[20] have made a similar point. As this is the region of the rotational distribution that will be paricularly sensitive to energetic constraints, the MHE representation is utilized throughout. The MHE appears to be an adequate representation of the potential for the purpose we employ here (it may not be sufficient were we to attempt to reproduce experimental rate constants for example) since inclusion of channel-dependent b_n reduction had little effect on the outcome of the MHE Monte Carlo calculations. This is very likely because the restrictions on those trajectories responsible for generating high b_n values when energy constraints dominate, are inherently contained in eq 3 and the four ellipsoid representation of the potential, though crude and simplistic, is sufficient to reproduce physical observables in a range of kinematic circumstances.

The method of calculation of RT cross sections is described fully in the paper by Marks[17] and further details, e.g. the operation of criteria by which each trajectory is judged to interact with a particular ellipsoid, may be obtained from there. The method has advantage over single HE models in that it allows

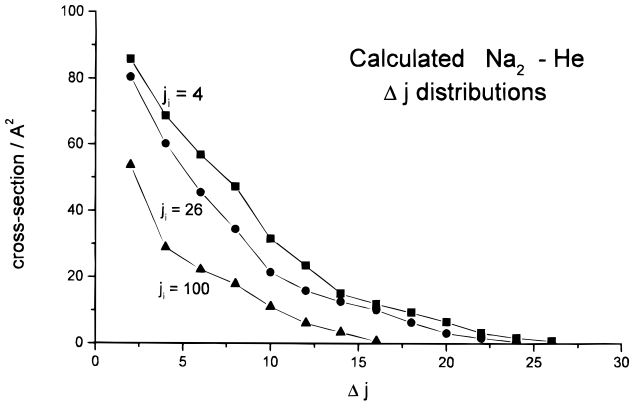

Figure 6. Results of MHE Monte Carlo calculations of Δj cross sections in Na_2*−He collisions for $j_i = 4$, 26, and 100. The plots demonstrate the rapid drop in RT efficiency as j_i increases.

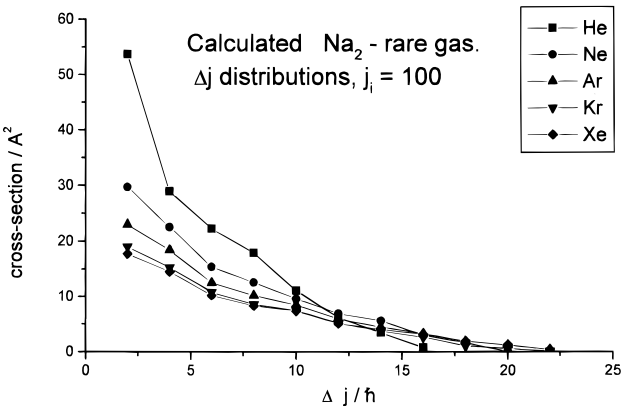

Figure 7. MHE Monte Carlo calculations of collision-induced Δj cross sections for Na_2*, $j_i = 100$ with each of the rare gases. The effect of increasing energy constraint in reducing b_n^{max} (and hence RT cross sections) as reduced mass increases, is clearly displayed in these plots.

more physical insight into the contributions of different regions of the potential to low, medium and high Δj channels and Marks has demonstrated[17] the importance of the outermost ellipsoids as major contributors to the low Δj cross sections. Calculations were based on the E + A equation representing simultaneous energy and AM conservation with $j_i \neq 0$ (eq 3). In the Monte Carlo simulations, 10^5 trajectories were used with velocity distribution represented by a Gaussian at the experimental temperatures reported by Brunner et al.[14]

The integral cross sections are given by

$$\sigma_{j_i \rightarrow j_f} = \frac{n(j_f)}{N} \pi (b^{max})^2 \qquad (5)$$

where $n(j_f)$ is the number of Monte Carlo trajectories resulting in final rotational state j_f and $b^{max}(=A)$ is the maximum impact parameter. This method, for four or more nested ellipsoids, yields accurate integral cross sections for (X)Na_2−He collisions over a wide range of energies[17]

Matching calculated cross sections with experimental data is not an objective here and this study is concerned with *changes* in the state-to-state RT cross sections as j_i and μ are varied to see if they follow predictions based on the velocity−AM plots. The potential surface utilized in the calculations remains the same for all rare gas collision partners and is the scaled (X)-Na_2−He potential. Four ellipsoids were used in all of the calculations reported here which yield a very reasonable exponential-like drop of cross sections with Δj. Ellipsoid dimensions were obtained from contours of the scaled potential using the method described by Marks.[17] The contours chosen varied somewhat from system to system in order that the highest energy ellipsoid matched the collision energy of the system concerned. However, all are representations (albeit rather rudimentary in form) of the same intermolecular potential.

Results and Discussion

We first investigate the influence of initial rotor state on RT cross sections as revealed by the nested ellipsoid-Monte Carlo calculations described in the previous section. Results from calculations on Na_2*−He are shown in Figure 6 where calculated state-to-state cross sections are shown for $j_i = 4$, 26, and 100ħ. The most striking feature is the fall in magnitude of each Δj and of total cross section across the series. Calculations on $j_i = 16$, 38, and 66ħ were also undertaken and the trends follow those shown in Figure 6.

This behavior as j_i increases was foreshadowed in v_r−Δj plots which indicate that for $j_i = 4$, all values of b_n up to the theoretical maximum (i.e., HBL) are permitted and thus RT is unconstrained by energetic restrictions. As j_i increases to 26ħ and beyond, restrictions on b_n revealed in Figure 3 indicate that RT cross sections for individual Δj channels will be reduced and furthermore the maximum attainable Δj will be diminished relative to data for $j_i = 4$. The calculated total cross section for $j_i = 100$ is much less than that for $j_i = 4$ and maximum Δj very much reduced. *Experimental* rate constants[14] follow the trends shown here very closely. Note that the distribution of rate constants and cross sections remains exponential-like despite the (sometimes severe) constraints on b_n arising from energy conservation. This is in significant contrast to cases in which there is a steplike energy boundary condition as in VRT for example[4,6] where the outcome is strongly diminished cross sections particularly in the low Δj region.

The influence of Xe on the j_i dependence of collision cross sections is considerably more dramatic than the example discussed above, a change well predicted by the v_r−Δj plots of Figure 5. We have not displayed the results of the MHE Monte Carlo calculations in graphical form since they follow trends shown in Figure 6 but have smaller values of cross section in all instances compared to those calculated with He as collision partner. The change with j_i is very noticeable in the experimental rate constants[14] where magnitudes fall by a factor of 4 or greater for each Δj channel as j_i changes from 4 to 66ħ.[14] MHE Monte Carlo calculations qualitatively reproduce this trend though the effect is not so marked as that reported experimentally. Thus, we can conclude from analysis of the v_r−Δj plots and the results of MHE Monte Carlo calculations that the change in the kinematic relationships when reduced mass is increased causes a major reduction in RT efficiency.

This reduction of RT efficiency as reduced mass increases, might initially seem counterintuitive since the relation $\Delta j = \mu v_r b_n$, which expresses the underlying physics of the RT mechanism, implies a process straightforwardly magnified by increasing μ. In terms of the simple physical picture that the AM approach to RT permits, collisions of specific relative velocity carry a greatly increased linear momentum when Xe is the partner compared, e.g., to He and this strongly influences the onset of energy constraint. In terms of the velocity−AM plots, the A equation is shifted to *lower* values of v_r for each Δj channel[13] when μ increases. Thus, for a given j_i the system becomes more likely to be influenced by energy constraints the larger μ becomes.

The effect of increased μ emerges from the MHE Monte Carlo simulations as shown in Figure 7 where calculated Δj state-to-

state cross sections are displayed for Na_2*, $j_i = 100\hbar$ interacting with each of the rare gas collision partners. Recall that in these calculations, the potential remains constant throughout. The four chosen ellipsoids represent contours of the same scaled (X)-Na_2−He potential of Schinke et al.[18] and therefore the steady reduction of RT cross sections as collision partner changes across the rare gas series from He to Xe is due to the variation in collision reduced mass. In reality of course the overall size of the potential will vary with collision partner and so experimental cross sections reflect changes in physical size of the collision partners. Very evidently the cross section for collision between Na_2 and Xe will greatly exceed that for Na_2−He encounters. Thus, absolute and relative magnitudes of the cross sections reported here are *not* an indication of what might be seen experimentally. It is the trend with change in reduced mass we have sought to isolate. As described in earlier sections, the effect of increased μ is to increase the dominance of energy constraint, forcing reductions in the maximum permissible value of b_n. This is manifest in reduced RT probabilities. In experimental data, changes in the intermolecular potential as μ increases may partially offset the mass effect.

The findings of this study, particularly in regard to the effect of $j_i > 0$ on RT cross sections, suggest that a reappraisal of the infinite order sudden (IOS) scaling law[21,22] may be appropriate. This widely used relationship which, at it simplest, takes the form

$$\sigma_{j_i \rightarrow j_f} = (2j_f + 1)\sum_l \begin{pmatrix} j_i & j_f & l \\ 0 & 0 & 0 \end{pmatrix}^2 \sigma_{0 \rightarrow l} \qquad (6)$$

allows cross sections for RT from any initial j state to be estimated from data taken from $j_i = 0$. The underlying physics of this equation fits well with the concept of LM → AM interconversion. However, it will be clear from the foregoing that the scaling relation as written above will be inaccurate in predicting cross sections for high j_i (though it should be reliable for all kinematic circumstances for which the dominant constraint remains the A relation with $b_n^{\max}$ = HBL).

The need to accommodate changing energy gaps for linear increase in Δj as j_i increases was recognized by DePristo et al.[23] who developed the energy corrected sudden (ECS) scaling law to correct for diminishing cross sections when $j_i \simeq 0$. The correction introduced in the ECS scaling relation is in terms of the number of radians of rotation, τ_j the diatomic undergoes throughout the "duration" of the collision and is defined by $\tau_j = l_c/v_{\text{rel}}$. In this, l_c is a characteristic "interaction length", i.e., the distance over which the intermolecular potential effectively acts, and is determined empirically. This leads to an "adiabatic factor" of the form

$$A_l^j = \frac{1 + \tau_l^2/6}{1 + \tau_j^2/6} \qquad (7)$$

which moderates the basic IOS scaling law. The work of Brunner et al.[14] demonstrates that this form of scaling, along with an empirical function for $\sigma_{l \rightarrow 0}$ can, with the appropriate choice of parameters, be used to fit a wide range of data. However, as Brunner et al. emphasize "...the lack of a simple theoretical justification (for their fitting laws)..." is a disquieting feature.

The development we have outlined here makes clear that the underlying kinematics of RT when $j_i \neq 0$ are considerably more complex than is portrayed in the IOS relationship. Our analysis indicates a strong dependence upon μ which is interwoven with the effect of $j_i \neq 0$. Furthermore, different Δj channels are affected differentially for a given j_i and μ. In this light, the energy correction to the IOS scaling law appears incapable of reflecting the physics of the dependence of RT cross sections on j_i. Collisional RT varies with initial rotor state and with reduced mass in a fashion that may be predicted quantitatively using eqs 1−3. It is not necessary to invoke poorly defined concepts such as the collision duration or the collision length and their introduction has led to interpretations of the variation of RT rate constants with j_i that might be regarded as misleading.

As we show, a more economical explanation of the j_i dependence of RT cross sections, and the variation with reduced mass, utilizes the straightforward notion of boundaries defined by energy conservation and their constraining influence on the linear-to-angular momentum interconversion mechanism. In this approach, there are no adjustable parameters and the effect of $j_i \neq 0$, and of changing reduced mass, are readily visualized and equally readily quantified. The impact of shifts in the energy conservation boundaries on the maximum value of b_n for individual channels may be incorporated into the rotational transfer function of Osborne and McCaffery[3] or, as we show here, left to MHE Monte Carlo calculations (with appropriate formulation of mechanism and boundary condition) to deal with.

The model we present in which the RT mechanism is *LM→AM* interconversion[2] has its roots in simple physical principles and the AM transfer function derived from this approach[3] utilizes parameters that are readily visualized. Energy conservation here, and in other recent publications,[3,4,6,13] constitutes a boundary condition that must be satisfied in order for the mechanism to operate. Under certain kinematic conditions, readily seen in velocity−AM plots, channel dependent reductions in the maximum value of b_n are enforced by the demands of energy conservation. These are readily quantified and may be incorporated into the transfer function for all j_i.

Conclusions

The principal objective of this work has been to seek to answer the question posed in the title, namely, ("*if the outcome of inelastic collisions is governed by kinematic factors), why are rotational distributions insensitive to kinematic differences?*" This is in the context of the many data sets examined by Clegg et al., who report that a wide range of collision partners yield very similar patterns of inelastic transfer behaviour. Rate constants for rotational transfer in Na_2* on collision with the rare gases provide a very striking demonstration of the similarities that exist despite change of almost an order of magnitude in collision reduced mass. We have not attempted to reproduce experimental data at this stage but have sought to clarify the physical principles underlying changes on RT rate constants and cross sections as collision conditions vary.

The approach has been through the AM theory of RT[2,3] in which the probability of RT is directly related to the probability of linear-to-angular momentum interconversion. This is principally kinematic in that input data are atomic masses, bond lengths, velocity distributions. However, the connection to dynamical factors is the requirement of a representation of the repulsive anisotropy (and its radial and angular dependence over the collision energy range). The operation of the LM → AM interconversion mechanism is most transparently revealed in plots of momentum (or, more usefully, relative velocity) against change in AM for threshold (channel opening) conditions corresponding to conservation of energy, of AM and of simultaneous energy and AM conservation. These are the eqs 1−3 above. They reveal the complex interplay of constraints

to the LM → AM process that arise from energy conservation when $j_i > 0$ and as collision reduced mass increases.

The $v_r-\Delta j$ plots reveal clearly that as j_i increases, energy constraints force a reduction of the maximum value of b_n for individual Δj channels and this has a direct impact on $\sigma_{j_i \rightarrow j_f}$, seen clearly in the transfer function, eq 4. The effect for high j_i may be considerable and its origin is the increase in the energy gap associated with a given AM change due to the quadratic dependence of rotational energy on j. The new upper limit to b_n is readily calculated. More relevant to the title question is the impact of increased μ. The variation with reduced mass is found to share similarities with change in j_i in that energy constraints become more and more intrusive as μ increases. The origin of this effect is rather different and arises from the increased linear momentum carried by the collision partners for a given relative velocity as reduced mass increases. This shifts the AM plot relative to the E plot, again with the net effect of a dominant energetic constraint with consequent limitations on maximum permitted value of b_n.

Multiellipsoid Monte Carlo calculations reveal how these effects are manifest under collision conditions where distributions of relative velocities typically are rather broad. The state-to-state cross sections for a given rare gas diminish rapidly as j_i increases. This finding and the physical relations upon which they are based brings to light problems inherent in variants on the IOS scaling relation and it is clear that corrections to the scaling relation that are based on collision duration which introduce the notion of a collision range are unnecessary and misleading. To model the effect of reduced mass change without other variables (e.g., size) changing we utilize a potential that is is unchanged for each rare gas. A series of four nested ellipsoids was constructed with dimensions taken from the contours of the potential. The calculations illustrates dramatically the kinematic basis of the diminishing efficiency of RT as μ increases.

To conclude, the physics of the RT process is greatly clarified through analysis of $v_r-\Delta j$ plots and Monte Carlo calculations. In a regime where the momentum interconversion mechanism is unconstrained by energy conservation boundaries, an increase in μ might be expected to lead to greatly enhanced RT. However, the requirement that the LM → AM mechanism operate at all times within the bounds of energy conservation counteracts this as j_i and μ increase through a process which limits the maximum value of b_n *for each channel*. *Absolute* values of state-to-state rate constants and cross sections may increase with increasing μ due to the changes in dimension of the collision partners but when normalized,[12] plots of $k_{j_i \rightarrow j_f}$ versus Δj for a given initial rotor state change only imperceptibly with collision partner.

Acknowledgment. We thank Prof. C. S. Parmenter and Dr. S. J. Clegg for bringing this aspect of kinematic models to our attention and for helpful discussions. We also thank EPSRC for an Advanced Fellowship (to A. J. Marks).

References and Notes

(1) Schiffman, A.; Chandler, D. *Int. Rev. Phys. Chem.* **1995**, *14*, 371.
(2) McCaffery, A. J.; AlWahabi, Z. T.; Osborne, M. A.; Williams, C. J. *J. Chem. Phys.* **1993**, *98*, 4586.
(3) Osborne, M. A.; McCaffery, A. J. *J. Chem. Phys.* **1994**, *101*, 5604.
(4) Clare, S.; Marks A. J.; McCaffery, A. J. *J. Chem. Phys.* **1999**, *111*, 9287.
(5) McCaffery, A. J.; Marsh, R. *J. Phys. Chem.*, accepted for publication.
(6) McCaffery, A. J. *J. Chem. Phys.* **1999**, *111*, 7697.
(7) Clare, S.; McCaffery, A. J. *J. Phys. B* **2000** *33*, 1121.
(8) Polanyi, J. C.; Woodall, K. *J. Chem. Phys.* **1972**, *56*, 1563.
(9) Brunner, T. A.; Pritchard, D. E. *Adv. Chem. Phys.* **1982** *50*, 589.
(10) McCaffery, A. J.; Wilson R. J. *Phys. Rev. Lett.* **1996** *77*, 48; *J. Phys. B* **1997**, *30*, 5773.
(11) Parmenter, C. S.; Clegg, S. M.; Krajnovitch, D. J.; Lu, S. P. *Proc. Nat. Acad. Sci. U.S.A.* **1997**, *94*, 8387.
(12) Clegg, S. M.; Burrill, A. B.; Parmenter C. S. *J. Phys. Chem. A* **1998**, *102*, 8477.
(13) Besley, N. A.; McCaffery, A. J.; Osborne, M. A.; Rawi, Z. *J. Phys. B* **1998**, *31*, 4267.
(14) Brunner, T. A.; Driver, R. D.; Smith, N.; Pritchard, D. E. *Phys. Rev. Lett.* **1978**, *41*, 856; *J. Chem. Phys.* **1979**, *70*, 4155. Brunner, T. A.; Smith, N.; Karp, A. W.; Pritchard, D. E. *J. Chem. Phys.* **1981**, *74*, 3324.
(15) Bosonac, S. *Phys. Rev. A* **1981**, *26*, 816.
(16) Kreutz, T. J.; Flynn, G. W. *J. Chem. Phys.* **1991**, *93*, 452.
(17) Marks, A. J. *J. Chem. Soc., Faraday Trans.* **1994**, *90*, 2857.
(18) Schinke, R.; Muller, W.; Meyer, W.; McGuire, P. *J. Chem. Phys.* **1981**, *74*, 3916.
(19) Korsch, H. J.; Ernesti, A. *J. Phys. B* **1992**, *25*, 3565.
(20) Korsch, H. J.; Schinke, R. *J. Chem. Phys.* **1981**, *75*, 3850.
(21) Mittleman, M. H.; Peacher, B. F.; Rozsnyai, B. F. *Phys. Rev* **1968**, *176*, 180.
(22) Goldflam, R.; Green, S.; Kouri, D. J. *J. Chem. Phys.* **1977**, *67*, 4149.
(23) DePristo, A. E.; Augustine, S. D.; Ramaswami, R.; Rabitz, H. *J. Chem. Phys.* **1979**, *71*, 850.